

# Full-fingerprint Volumetric Subsurface Imaging using Fourier-Domain Optical Coherence Tomography

Ctirad Sousedik

Norwegian University of Science and Technology (NTNU)  
Teknologiveien 22, 2815 Gjøvik, Norway  
ctirad.sousedik@ntnu.no

Ralph Breithaupt

Federal Office for Information Security (BSI)  
Postfach 20 03 63, 53133 Bonn, Germany  
ralph.breithaupt@bsi.bund.de

**Abstract**—Despite the long history of automated fingerprint recognition, the state-of-the-art 2D sensors still struggle with abraded, dry, wet or greasy fingers, as well as extra-soft skin of the infant fingerprints. But above all, the current sensors suffer from vulnerabilities to presentation attacks, which greatly limits their applicability in unsupervised scenarios such as border control. Optical Coherence Tomography (OCT) represents an alternative approach with a high potential to address the existing challenges. In this paper, we present a novel fingerprint sensor based on Fourier Domain Optical Coherence Tomography (FD-OCT), capable of capturing a 3D volumetric full fingerprint scan from a 2x2cm area, along with subsurface details such as sweat glands and the internal fingerprint. The novelty of our setup lies in the ability of FD-OCT-scanning a full 3D volumetric fingerprint at high-resolution at speeds that demonstrate the usability of 3D OCT in real-world applications.

## I. MOTIVATION

In the recent years, biometrics are becoming an integral authentication mechanism in IT security devices. Unlike passwords, which are difficult to remember and can easily be forgotten, and access cards, which can be misplaced, biometrics offer means of authentication that are convenient and always available.

Among the range of biometric modalities developed and practically applied, face and in particular fingerprint recognition are currently predominant. Despite its three-decade long history, unresolved technical issues still exist that significantly reduce the applicability of fingerprint recognition for multiple important scenarios:

- Worn out fingers - The fingerprint can be abraded or significantly damaged on the surface for occupations like chemists, guitar players, construction workers etc.
- Wet or greasy fingers - the surface liquid fills the fingerprint valleys upon touching the fingerprint sensor surface - decreasing the fingerprint quality often to completely unusable levels
- Infant fingerprints - infant fingerprint skin is too soft and flattens on the sensor surface - which limits usability of fingerprints to fight child trafficking

In addition, similarly to majority of biometric modalities, fingerprint recognition can be subjected to spoofing attacks.

Especially for the case of fingerprints, the artifact fingerprints can be made of inexpensive materials using simple techniques [1][2].

Despite the large body of research on this problem of presentation attack detection (PAD), there is no fingerprint sensing technology yet capable of universally addressing these challenges, especially for the cases of novel artificial fingerprint materials and production techniques[1]. The existing PAD approaches applied in the industry are based on multi-spectral imaging or on a large amount of additional single-purpose sensors that require machine learning approaches to take the PAD decision. This makes them vulnerable to novel unexpected approaches not considered in the training process[1].

### A. OCT fingerprinting

Due to limitations of the existing 2D fingerprint sensing technologies, especially regarding PAD, the research community has been considering alternative sensing technologies that would provide PAD-related cues in much more readily fashion.

One of the promising alternative scanning approaches with a large PAD potential is the Optical Coherence Tomography (OCT). The application of OCT for fingerprints sensing comes with a promise of large improvements, addressing many of the current challenges. The OCT is capable of capturing a 3D volumetric representation of the fingertip skin up to a maximum depth of 2-3mm, in a fashion that does not require contact with a surface. This property offers great advantages for scanning wet or greasy fingers or the extra-fine infant fingerprints. In addition, the OCT captures the internal structure of the fingertip skin such as sweat glands and the internal fingerprint - a subsurface cell structure identical to the surface fingerprint and responsible for its stability and regeneration. The ability to scan the internal fingerprint offers great promise for scanning fingers with abraded or temporarily damaged surface fingerprints. Last but not least, the OCT offers great promise regarding the very challenging issue of a PAD capable of handling novel unexpected artifact fingerprints. The ability to capture the inner fingerprint, the sweat glands and a general light scattering profile of the human

finger tip skin arguably provides more, more readily available, PAD-relevant information than the existing 2D sensors.

However, along with its many advantages, OCT as a novel technology fingerprinting comes with a number of challenges associated with a step from 2D to 3D scanning. The data amounts generated by 3D scanning at high-resolution are significant, and require novel scanning & processing approaches to provide for authentication in a matter of seconds (e.g. less than 6s total for a border control application)

## II. RELATED WORK

With a few exceptions, the existing research regarding OCT fingerprinting focuses on using existing OCT setups and addressing the signal processing challenges, rather than development of a specific-purpose OCT fingerprint sensor.

The initial studies regarding application of the OCT for fingerprints, focusing specifically on the PAD, was carried out by Cheng & Larin [3][4] and Peterson & Larin[5]. They proposed a OCT setup capable of capturing 2D in-depth scans of fingertip skin area, and suggested techniques to utilize the in-depth information for fake finger detection. In addition, Nasiri-Avanaki et al. [6] have also suggested a 2D in-depth slices acquired by OCT as a suitable path to develop fingerprint PAD. Liu and Buma [7] have experimented with a FD-OCT setup capable of capturing a 3D OCT volume from a partial fingerprint area, and suggested the positions sweat glands as a possible biometric characteristic. Bossen et al. [8] have experimented with capturing a partial fingerprint area using a commercially available OCT setup and pointed out the possibility of capturing the internal fingerprint. Cimalla et al. [9] have developed a high-resolution FD-OCT setup capable of capturing a volumetric representation from small area of the fingerprint. They have clearly visualized the helix structure of the sweat-glands, observable with their high-resolution OCT. In the framework of the OCT-I project, Meissner et al. [10] have used an FD-OCT setup to collect a large scale dataset of genuine and fake volumetric fingerprint OCT scans from a small area of 4x4mm and carried out a manual classification study to assess the PAD potential of the OCT for various fake materials & production techniques.

Khutlang et al.[11] have used a commercially available FD-OCT scanner to capture a partial fingerprint area and experimented with internal fingerprint detection and subsequent feature extraction.

Promising recent studies by Darlow et al. [12][13][14] focus on the fast extraction of the 2D internal and surface fingerprints from 3D volumetric fingerprint scans. Their studies are carried out using a commercially available FD-OCT setup capable of scanning in a 15x15mm fingerprint area.

Regarding an effort to develop a specific-purpose fingerprint OCT sensor, with a scanning area sufficient for reliable fingerprint identification, Auksorius & Boccaro [15][16] have taken an approach using Full-Field (FF) OCT in the framework of the INGRESS project[17]. Unlike the FD-OCT OCT setups, which separately capture in-depth scan-lines at high speed, the FF-OCT captures a 2D image at once, from a single specific

depth using a 2D camera. This approach requires pressing the fingerprint against a glass surface, so that the curvature of the surface and internal fingerprint is flattened. According to earlier studies[10][18], this comes with disadvantages regarding fingerprint scanning under difficult conditions (dry, wet, greasy fingers etc.) similar to those faced by the existing 2D sensors. In addition, the readily 2D information extracted from the finger does not contain as many PAD-related cues as a full 3D volumetric scan, even though it leads to smaller data amounts and as such carries the potential for faster operation. The initial efforts to develop a full volumetric fingerprint scanner have been carried out by Breithaupt et al.[19] in terms of the OCT-II, however, the originally proposed design did not meet the imaging quality requirements necessary for clear visualization of the finer internal structures such as sweat glands.

## III. OCT FINGERPRINT SCANNER SETUP

Our fingerprint scanner setup is based on the Fourier-Domain (FD) OCT imaging technique as illustrated by Fig. 1.

### A. *FD-OCT scanning*

The illumination is generated by a super-luminescent diode (SLD), operating in an infra-red spectral band of 800-900 nm, coupled into a fiber optic arm of a fiber-optic coupler with a splitting ratio of 50:50. The light travels via the fiber-optic coupler into the scanning head, where it is collimated into a light beam with diameter of 3.9mm. The light travels from the fiber-optic collimator into a 50:50 beam splitter, such that 50% of the light travels through with unchanged trajectory as the sample beam and 50% of the light is deflected at a 90° angle into the reference arm as the reference beam.

The sample beam is deflected by a setup of 2 mirror galvanometers, which enable deflection of the beam in two orthogonal axes. The deflected sample beam is then focused by an objective lens system, such that for any deflection setting of the mirror galvanometers in a certain range, the beam leaves the lens in a vertical direction and is point-focused at a distance from the objective, which equals to its focal length.

In a limited distance range from the point of focus, the sample beam is sufficiently narrow to allow for the high-resolution imaging purposes. The narrowed sample beam travels into the scanned finger and is scattered both on its surface and in the skin underneath its fingerprint surface. A certain portion of the scattered light is reflected back as rays taking the exact same range of trajectories that have been taken by the rays of the sample beam itself, which re-couples the light back into the optical setup, deflecting the light rays, re-reflected back from the finger, into the same optical elements in reverse order.

In the reference arm, the reference beam leaves the beam splitter and is reflected back into the system, after having its intensity significantly reduced by an adjustable setup. This intensity reduction setup allows to match the strongly reduced intensity range of the sample light that has been scattered in the finger, and as such only partially reflected back into the optical setup.

The sample beam, back-reflected from the finger, and the reference beam - after their re-coupling in the beam splitter - optically interfere. The interfered re-combined light travels back into the fiber-optic coupler and is measured by a spectrometer operating in the appropriate range of 800-900 nm.

A single measurement taken by the spectrometer allows to obtain a 1D depth profile,  $d(z)$ , of the scattering properties of the scanned finger, at the current position of the sample beam, in the following manner. The spectrometer records a spectral profile  $p(\lambda)$ , where  $\lambda$  is the wavelength in the range of 800-900 nm. If no finger is present, no sample light is back-reflected into the system, and the profile  $p(\lambda)$  equals to the spectral profile of the back-reflected reference light  $p_r(\lambda)$ . If a scanned finger is present, the specific measured intensities in the interference profile,  $p(\lambda)$ , equal to the reference spectral profile altered by the interference pattern,  $f(\lambda)$ , due to interference of the reference light with the back-reflected sample light:

$$p(\lambda) = p_r(\lambda) + p_i(\lambda) \quad (1)$$

By subtraction of the reference spectral profile,  $p_r(\lambda)$ , from the measured spectral profile  $p(\lambda)$ , it is possible to obtain the interference pattern  $p_i(\lambda)$  - which depends primarily on the scattering properties of the scanned finger in the currently measured depth profile,  $d(z)$ .

In order to obtain the depth profile  $d(z)$ , the wavelength-dependent intensities  $p(\lambda)$  must be transformed into frequency-dependent intensities  $p_i(f)$ . The depth profile  $d(z)$  equals the modulus of Fourier transform of the interference pattern  $p_i(\lambda)$ .

$$d(z) = |\mathcal{F}(p_i(f))| \quad (2)$$

Intuitively, for all sample illumination waves of wavelength  $\lambda$ , the reflected wave is a superposition of the waves as reflected from the entire depth profile of the scanned sample - the reflected wave represents a complex number determined by the integral of the illumination wave and the entire depth profile of the finger. During the interference with the reference beam, the measured intensity  $p(\lambda)$  is increased or decreased by interference with the reflected wave by  $p_i(\lambda)$  - the real part of the complex integral. As such, a set of measured intensity changes for different wavelengths  $\lambda$  represents the real numbers resulting from a Fourier transform of the scanned depth profile.

The inevitable loss of the complex part of the Fourier transform  $\mathcal{F}(d)$  does not allow for unambiguous reconstruction of the depth profile  $d$ . In practice, the scanned sample is positioned above the focal plane only, which is equivalent to a depth profile with the first half equal to 0. Such a depth profile can be reconstructed unambiguously at 1/2 of the spectrometer's resolution.

### B. 3D volumetric data acquisition

In order to obtain a 3D volumetric representation of the entire fingerprint, a depth profile  $d(z)$  has to be acquired for each  $x$  and  $y$  coordinate of the scanning area.

An analog waveform  $V_x(t)$  resp.  $V_y(t)$  is generated by an analogue signal generator for each of the axes  $xy$ . For each axis  $xy$ , the momentary voltages in the waveform represent a specific rotation of the the mirror galvanometer at a specific point in time  $t$  - allowing to sequentially set specific  $xy$  coordinates of the scanning beam.

A shared synchronization clock is used to activate the camera shutter of the spectrometer as well as generation of a next sample  $V_x(t), V_y(t)$ , which adjusts the position of the mirror galvanometers into a new  $xy$  coordinate via a controller circuit.

The programmable analog waveform generator allows for the  $xy$  coordinates of the sample beam to be chosen in software, which allows for software-controlled adjustments of both the lateral resolution and the scanning area of our setup.

### C. Scanning head

In our setup, the fingerprint is scanned free-air, as opposed to pressing the finger against a surface, such as glass[15]. This design feature results from the findings in earlier studies, which have shown that scanning the finger pressed against a glass surface mitigates the ability of the OCT scanner to capture the surface fingerprint under difficult conditions (wet, greasy, etc. fingers) in a very similar fashion to existing 2D sensing technologies[18][10].

Our scanning head, illustrated by Fig. 2, allows to rest the finger, while simultaneously leaving the fingerprint area in free-air. This design allows the OCT scanner to capture a 3D volumetric representation of the finger, without having to deal with loss of the fine fingerprint structure due to the pressing the finger against a flat surface.

In the current design, the module of the scanning head contains the beam collimator, beam splitter, the reference arm, the galvanometers and the lense objective.

### D. Main & processing module

Currently, the main module contains the SLD light source, the spectrometer and the FPGA-based control circuitry necessary for real-time synchronization of the movement of the mirror galvanometers and the shutter of the spectrometer. The main module is connected to a PC unit with a GPU for processing & visualization purposes.

During the scanning, the spectrometer transfers 2048 pixels measurements at a 12-bit precision with a line-rate of 100 kHz over a CameraLink interface to the RAM of the processing PC - this gives a throughput of about 293 MB/s. This allows, together with the waveform generators operating at 100 kS/s, to capture a volumetric scan of the fingerprint at a lateral resolution of 512 DPI in our 2x2 cm scanning area in 1.63 s.

## IV. TESTING & RESULTS

A significant challenge associated with 3D volumetric scanning of the fingerprint lies in the generated data amounts. During the operation, the spectrometer of 100 kHz line-rate and 2048 pixels per lines rate generates - 100K x 2048 x 12bit - about 293 MB/s of data, where each scan-line needs

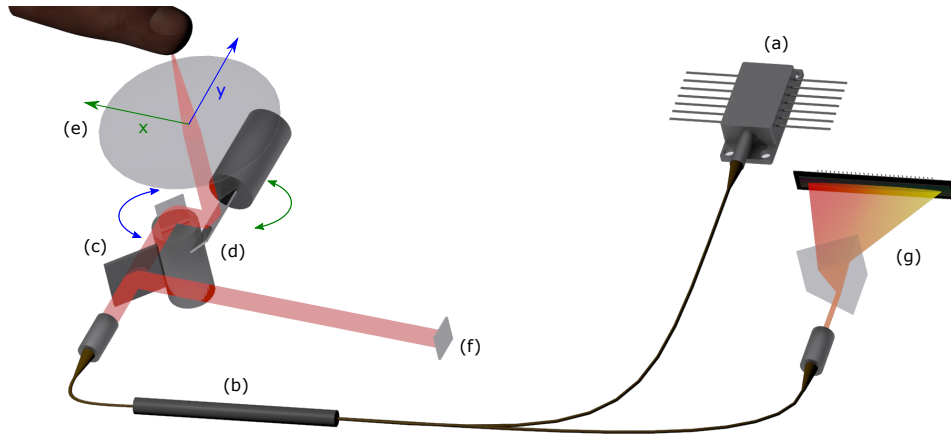


Fig. 1. Schematic depiction of our FD-OCT fingerprint scanner: (a) SLD 800-900 nm light source, (b) fiber coupler, (c) beam splitter, (d) mirror galvanometers, (e) objective lens(es), (f) reference arm back-reflector, (g) 800-900 nm spectrometer

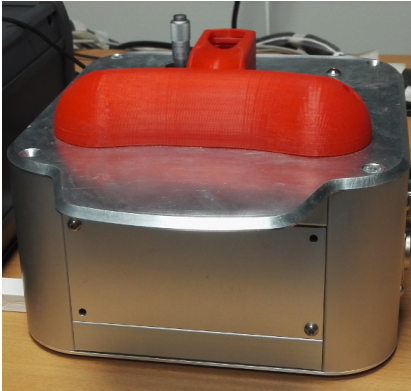


Fig. 2. Scanning head of the FD-OCT fingerprint scanner

to be processed by Fourier Transform in order to obtain the depth profile  $d(z)$ . In our current setup, a single core i7 processor in the PC module processes the data in a multi-threaded pipeline during the scanning process itself, able to perform the FFT inversion slightly faster than the spectrometer generates the raw data. As such, the pipelined FFT inversion provides a readily processed spatial volumetric representation of the fingerprint practically immediately after the end of the scanning process.

In comparison with related attempts for OCT-based subsurface fingerprint scanning using FF-OCT[15], our FD-OCT setup allows for software adjustments of the scanning resolution. This allows to perform a lower-resolution scan of the entire fingerprint (1.63 s at 512 DPI, current standard fingerprint resolution), extracting the surface fingerprint and subsurface fingerprint, allowing for superior reliability under difficult conditions (dry, wet, greasy fingers etc.). Immediately afterwards, a higher-resolution scan of a partial area can be acquired, for the purposes of reliable detection of fake fingerprints - PAD.

### A. Scanner software

In order to allow for reliable acquisition of the fingerprint volume with correct positioning of the finger, the sensing software is equipped with a preview mode. Under the preview mode, the scanner repeatedly scans a low-resolution volume of  $128 \times 128 \times 1024$  voxels with an area of  $2 \times 2$  cm and the volume is readily FFT-processed in a pipeline visualized using a GPU at semi-realtime speed of 5 scans per second.

In the high-resolution scanning mode, the software allows for a pipelined FFT-inversion and immediate visualization of the scanned volume using a GPU as well.

### B. Collected dataset

To evaluate our fingerprint scanner setup and open up for the possibility future research of the behavior and properties of the OCT scans of human fingerprints, we collected the following dataset:

- fingerprint volume of  $1408 \times 1408 \times 1024$  voxels
- $2 \times 2$  cm scanning area
- $14.2 \mu m$  lateral resolution
- 700 fingers
- 70 participants
- all 10 fingers per participant

A single volumetric scan of a finger in this dataset, in order to open for the possibility of offline research of the FFT processing pipeline as well, requires for storage of  $2048 \text{ pixels} \times 1408 \times 1408 \times 12 \text{ bit}$  (stored as 16bit) - 7,7 GB of raw spectral data. In addition, the processed spatial data, readily available upon the end the scanning, are stored -  $1024 \times 1408 \times 1408 \times 8 \text{ bit}$  - 1.9 GB. This results in a total dataset size of - 700 fingers  $\times$  9.7 GB - 6.8 TB.

From an identical set of participants, 2D fingerprints of 50 participants from all 10 fingers have been collected using a standard optical 2D sensor, in order to allow for studies of compatibility of the OCT fingerprints and the standard 2D fingerprints.

In addition, a following high-resolution dataset of partial fingerprints has been collected, to enable for a study of human skin behavior under high-resolution OCT, primarily for the purpose of fake fingerprint detection (PAD):

- fingerprint volume of 512 x 512 x 1024 voxels
- 3.58 x 3.58 mm scanning area
- 7  $\mu\text{m}$  lateral resolution
- 150 fingers
- 50 participants
- index, ring and little finger per participant

Despite the relatively large data sizes, our experiments indicate the speed of the computer RAM, the Cameralink interface and further processing on GPUs (320 GB/s raw data throughput for standard gaming GTX 1080) would allow for scanning & processing speeds necessary for acquisition and processing in a matter of seconds at medium resolutions.

OCT scans captured by our setup are visualized by Fig. 3-5. Fig. 3 and Fig. 4 represent a 3D transparent visualization of an index finger resp. thumb. The sweat glands are visible under the transparent-rendered surface fingerprint.

Visualization of the surface fingerprint, sweat glands along with the internal fingerprint layer are shown by Fig. 5. A vertical cut through a fingerprint scanned from a 2x2cm area is illustrated by Fig. 5a, while Fig. 5b represents an identical fingerprint, visualized from the side as a highly-transparent 3D volume. Fig. 5c represents a vertical cut through a partial fingerprint from a 3.58x3.58mm area.

## V. CONCLUSION AND FUTURE WORK

We have developed a novel specific-purpose FD-OCT fingerprint sensing setup. Unlike existing designs, our setup is capable of imaging a full fingerprint from a 2x2 cm area, as a complete volumetric representation at speeds that demonstrate the usability of 3D OCT in real-world applications.

Our setup allows for software adjustments of the scanning area & resolution, which opens up the possibility for a 2-stage scanning pipeline - fingerprint extraction at lower resolutions and high-resolution limited-area scanning for PAD purposes.

The future work would involve optimizations of the setup regarding the scanning range & resolution through the air as well as imaging depth into the fingertip skin, by an improved light management via non-evenly-splitting beam splitters and fiber couplers and related possible changes of the beam diameter.

The scanning head of the setup should be further improved to better address the issues associated with involuntary muscle shakes, that pose a challenge for high-quality imaging.

The future efforts will also focus on miniaturization, by replacement of the relatively large general-purpose electronics responsible for the galvanometer control and camera synchronization, by a much smaller specialized solution. The scanning head can be significantly miniaturized by usage of a MEMS mirror system in replacement of the mirror galvanometer pair.

We are also currently experimenting with a solution for segmentation of the surface & internal fingerprint at acceptable

processing times - a problem that has been recently addressed in a promising fashion by Darlow et al.[12].

## ACKNOWLEDGMENT

The funding for this research was provided in terms of the BSI project OCT-DATA.

## REFERENCES

- [1] C. Sousedik and C. Busch, "Presentation attack detection methods for fingerprint recognition systems: a survey," *IET Biometrics*, vol. 3, no. 4, pp. 219–233, 2014.
- [2] V. Mura, L. Ghiani, G. L. Marcialis, F. Roli, D. A. Yambay, and S. A. Schuckers, "Livdet 2015 fingerprint liveness detection competition 2015," in *Biometrics Theory, Applications and Systems (BTAS), 2015 IEEE 7th International Conference on*, Sept 2015, pp. 1–6.
- [3] Y. Cheng and K. V. Larin, "Artificial fingerprint recognition by using optical coherence tomography with autocorrelation analysis," *Appl. Opt.*, vol. 45, no. 36, pp. 9238–9245, 2006.
- [4] Y. Cheng and K. Larin, "In Vivo Two- and Three-Dimensional Imaging of Artificial and Real Fingerprints With Optical Coherence Tomography," *Photonics Technology Letters, IEEE*, vol. 19, no. 20, 2007.
- [5] L. E. Peterson and K. V. Larin, "Image classification of artificial fingerprints using Gabor wavelet filters, self-organising maps and Hermite/Laguerre neural networks," *International Journal of Knowledge Engineering and Soft Data Paradigms*, vol. 1, no. 3, Oct. 2009.
- [6] M.-R. Nasiri-Avanaki, A. Meadway, A. Bradu, R. M. Khoshki, A. Hojjatoleslami, and A. G. Podoleanu, "Anti-Spoof Reliable Biometry of Fingerprints Using En-Face Optical Coherence Tomography," *Optics and Photonics Journal*, vol. 1, no. 3, pp. 91–96, 2011.
- [7] M. Liu and T. Buma, "Biometric Mapping of Fingertip Eccrine Glands With Optical Coherence Tomography," *Photonics Technology Letters, IEEE*, vol. 22, no. 22, pp. 1677–1679, Nov 2010.
- [8] A. Bossen, R. Lehmann, and C. Meier, "Internal Fingerprint Identification With Optical Coherence Tomography," *Photonics Technology Letters, IEEE*, vol. 22, no. 7, pp. 507–509, 2010.
- [9] P. Cimalla, J. Walther, M. Mehner, M. Cuevas, and E. Koch, "Simultaneous dual-band optical coherence tomography in the spectral domain for high resolution in vivo imaging," *Opt. Express*, vol. 17, no. 22, Oct 2009.
- [10] S. Meissner, R. Breithaupt, and E. Koch, "Defense of fake fingerprint attacks using a swept source laser optical coherence tomography setup," in *Proc. SPIE, Frontiers in Ultrafast Optics: Biomedical, Scientific, and Industrial Applications*, vol. 8611, 2013.
- [11] R. Khutlang, N. P. Khanyile, S. Makinana, and F. V. Nelwamondo, "High resolution feature extraction from optical coherence tomography acquired internal fingerprint," in *2016 17th IEEE/ACIS International Conference on Software Engineering, Artificial Intelligence, Networking and Parallel/Distributed Computing (SNPD)*, May 2016, pp. 637–641.
- [12] L. N. Darlow, J. Connan, and A. Singh, "Performance analysis of a hybrid fingerprint extracted from optical coherence tomography fingertip scans," in *2016 International Conference on Biometrics (ICB)*, June 2016, pp. 1–8.
- [13] L. N. Darlow, J. Connan, and S. S. Akhoury, "Internal fingerprint zone detection in optical coherence tomography fingertip scans," *Journal of Electronic Imaging*, vol. 24, no. 2, p. 023027, 2015.
- [14] L. N. Darlow and J. Connan, "Efficient internal and surface fingerprint extraction and blending using optical coherence tomography," *Appl. Opt.*, vol. 54, no. 31, pp. 9258–9268, Nov 2015.
- [15] E. Auksorius and A. C. Boccara, "Fingerprint imaging from the inside of a finger with full-field optical coherence tomography," *Biomed. Opt. Express*, vol. 6, no. 11, pp. 4465–4471, Nov 2015.
- [16] —, "Internal fingerprint imaging with visible light full-field optical coherence tomography," in *Biomedical Optics 2016*. Optical Society of America, 2016.
- [17] "EU-project INGRESS." [Online]. Available: <http://www.ingress-project.eu/>
- [18] S. Meissner, R. Breithaupt, and E. Koch, "Fingerprint fake detection by optical coherence tomography," pp. 85 713L–85 713L–4, 2013.
- [19] R. Breithaupt, C. Sousedik, and S. Meissner, "Full fingerprint scanner using optical coherence tomography," in *Biometrics and Forensics (IWF), 2015 International Workshop on*, March 2015, pp. 1–6.



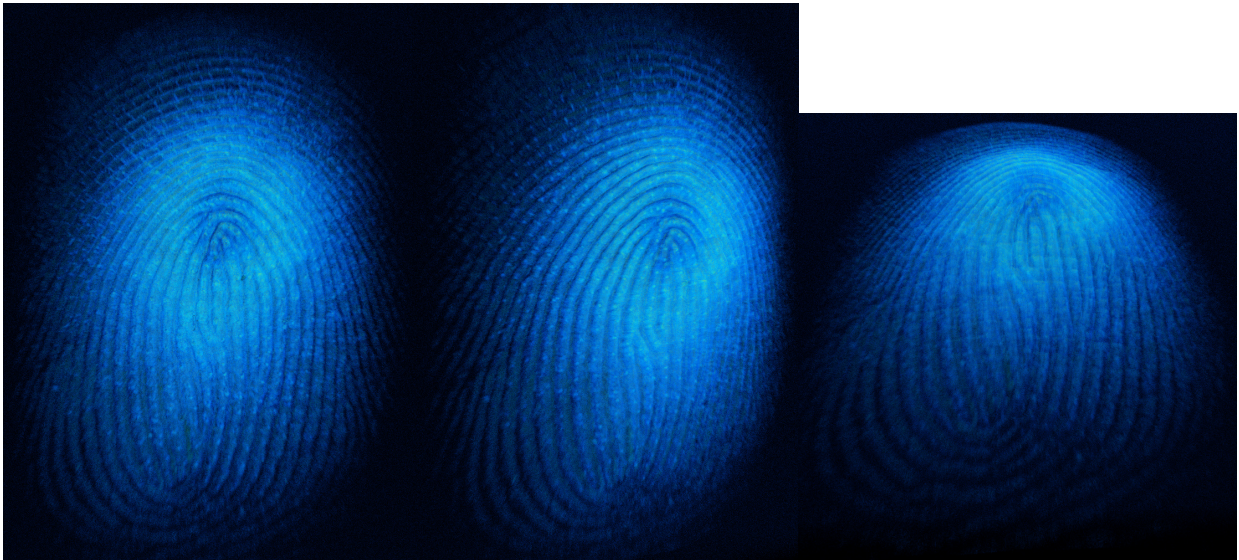


Fig. 3. index finger scan: 2x2cm area, 1408x1408x1024, 14.2 $\mu$ m - surface fingerprint & sweat glands - transparent 3D visualization



Fig. 4. thumb scan: 2x2cm area, 1408x1408x1024, 14.2 $\mu$ m - surface fingerprint & sweat glands - transparent 3D visualization

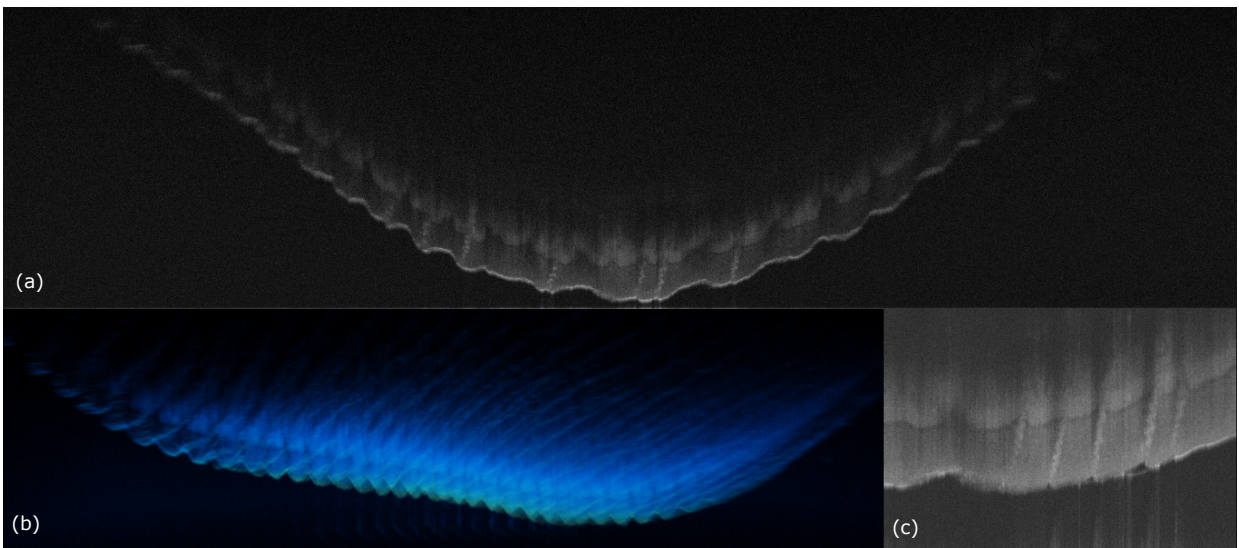


Fig. 5. thumb scan: (a) 2x2cm area, 1408x1408, 14.2 $\mu$ m, 5 averaged slices; (b) 3.58x3.58 area, 1408x1408, 14.2 $\mu$ m transparent 3D visualization; (c) 3.58x3.58 area, 512x512, 7 $\mu$ m, 10 averaged slices